# Monte Carlo Simulations of X-ray Generation to Analyse Scintillator Spectrometer.

**Contact:** dean.rusby@stfc.ac.uk

**D. R. Rusby**
*Central Laser Facility,*
*STFC Rutherford Appleton Laboratory,*
*Harwell Campus, Didcot*
*OX11 0QX, United Kingdom*

**D. Neely**
*Central Laser Facility,*
*STFC Rutherford Appleton Laboratory,*
*Harwell Campus, Didcot*
*OX11 0QX, United Kingdom*

**C. Brenner**
*Central Laser Facility,*
*STFC Rutherford Appleton Laboratory,*
*Harwell Campus, Didcot*
*OX11 0QX, United Kingdom*

**C. Armstrong**
*Department of Plasma Physics,*
*University of Strathclyde,*
*Glasgow G4 0NG, United Kingdom*

## Abstract

The temperature of fast electrons in laser-solid interactions is often difficult to determine due to the electrostatic fields present on the front and rear surface. The Bremsstrahlung x-rays emitted from these interactions are directly linked to the temperature of the internal hot-electron population. Here we discuss the simulations that are conducted using GEANT4 that enable the temperature extraction of electron temperatures using a using a scintillator based x-ray spectrometer.

## 1 Introduction

The temperature/spectrum of the hot electron population that is accelearted into a solid target is of great interest, however the direct diagnosis is extemely difficult due to the large electrostatic forces involves. X-rays produced from laser-solid interactions are of much interest as they are instrincally link to the hot electorn population that is their source. From the emitted x-ray signatures, it is possible to infer the electron temperature.

For a number of years, a scintillator based absorption x-ray spectrometer has been deployed in the Central Laser Facility (CLF) in order to measure the x-rays emitted from solid target experiments [6]. The main advantage of this diagnostic compared to similar diagnostics is that it instantly digitises the data and is able to operate at much higher repetition rates than current laser systems in the CLF. In order to take advantage of these capabilities, a number of simulations have been conducted and programmes have been developed to aid the analysis the experimental data taken using the diagnostic.

In this report, we will discuss in detail different techniques that are used to analyse the data and determine the hot electron temperature within a solid target.

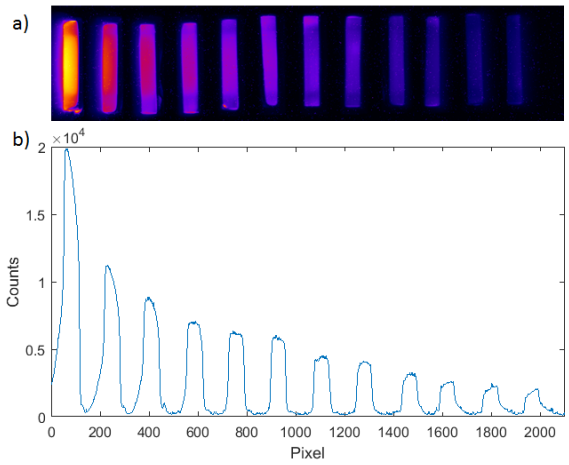


Figure 1: a) Example data from the scintillator based x-ray spectrometer. The x-rays are entering from the left and being absorbed as they pass through the array. The photons that are emitted are recorded on a camera. b) shows a lineout of the image. The signal clearly falls as a function of layer.

## 2 Diagnostic Overveiw

The diagnostic is based on a 1D array of scintillators. As the x-ray pass through the scintillators, they are absorbed. The higher energy x-rays with be able to transmit further into the array in comparison to the lower energy x-rays. The ammount of light emitted by the scintillator is proportional to the energy absorbed. An example of the output from the diagnostic is shown in Figure 1. The sensitivity of the any particular arrangement to different energy of x-rays is determined by the response function; which is discussed in section 3.1 (an example is shown in Figure 3).

The design of the scintillator absorption spectrometer has gone through a number of design iterations. Currently the design is as shown in Figure 2. A lead housing allows for position of the diagnostic to be permanent whilst the array housing is 3D printed and interchange-

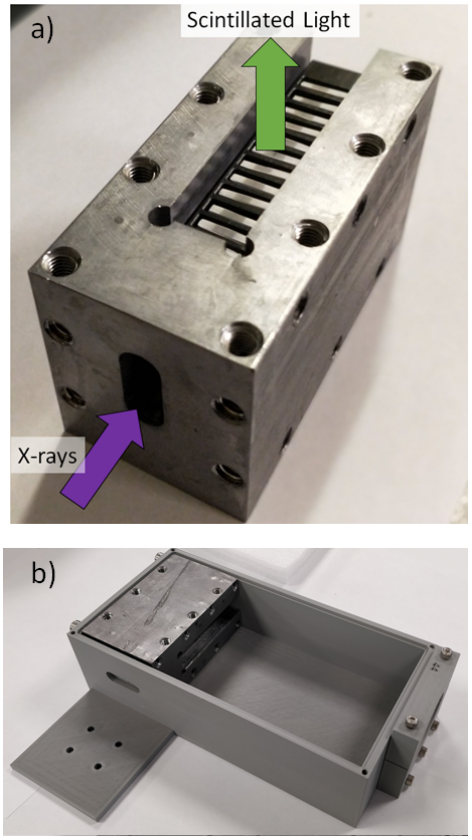


Figure 2: a) Picture of the current diagnostic. The scintillators are wrapped and place in a 3D printed holder. The holder in then placed in a Lead shield that apodisors the x-rays. The scintillation light is emitted in one direction and recorded on a camera. b) The 3D printed plastic casing that provides mounting for a lens and is light tight.

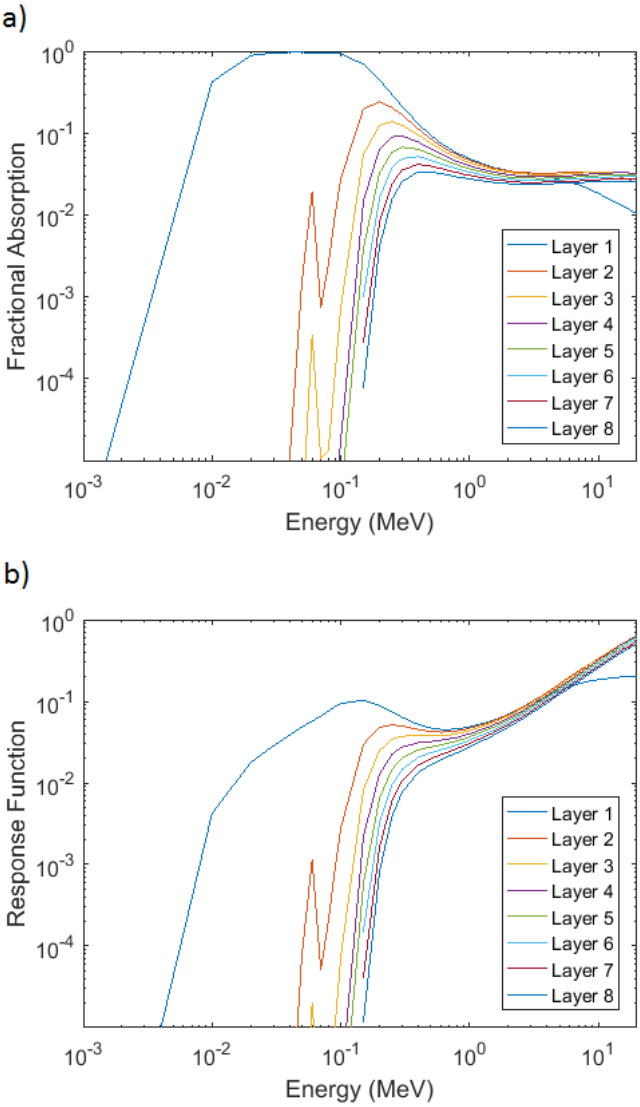


Figure 3: a) The fractional absorption of the an example scinatillor array. b) The response function of the same example scintillator arrangement.

able. The lead housing is then housed in a 3D printed box that ensures the diagnostic is light tight and that the imaging system is consistent across different setups, as shown in Figure 2 b).

## 3 Simulations

To determine the x-ray spectra and electron temperature, we need to conduct two simulations: one to determine the response function and the x-ray spectra from different solid targets. The response function determines the sensitivity of the diagnostic and can be multipled by a x-ray spectrum to calculate the energy absorbed, which as previously mentioned, is proportional the light emitted. if we multiply a simulated x-ray spectrum by the response function, we can compare this output by the experimental output; the closest match will determine the hot electron temperature. This will require us to run many simulations to create as many x-ray spectra as possible.

The following section will discuss each separately in there own sections. Firstly a brief outline of the chosen Monte Carlo code GEANT4 will be given, with the methods that are used run and batch simulations.

GEANT4 is capable of simulating all the relevant physics that are required for the x-ray generation [7]. It comes with standard electromagnetic physics list (called standardEM) and also custom ones which are specialised in different energy regions or physical processes. The two that are applicable to this work are Penelope and Livermore packages [8–11], which are both specialised to work in the 'low-energy' region (100's eV to 10's MeV).

GEANT4 is able to be parallelised across many cores, however, the simulations we are conducting here require $10^8$ iterations at most. With this number of events, a single CPU core can complete the simulation in minutes. The system we currently employ uses a python script to

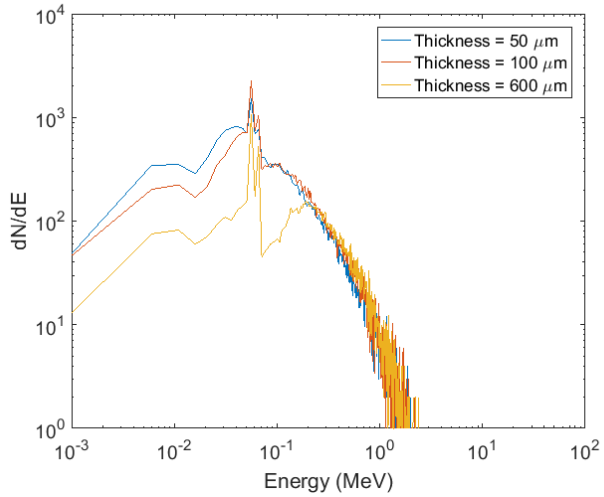


Figure 4: The x-ray spectrum generated in GEANT4 for three different thicknesses of Ta using an input of 350 keV electron spectrum.

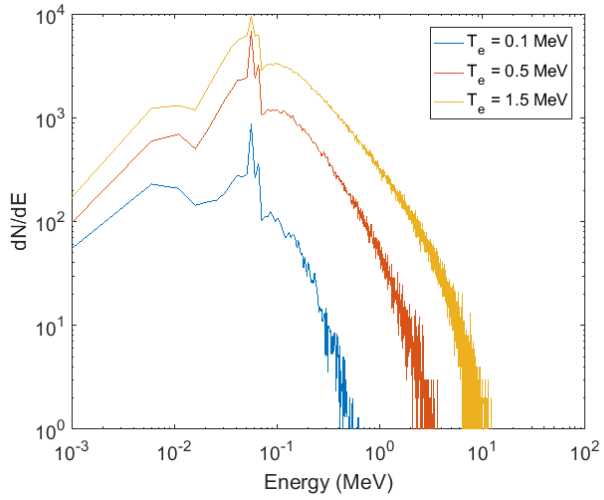


Figure 5: The x-ray spectrum generated in GEANT4 for three different temperatures of electron distributions using a 100 $\mu$m Ta target.

queue many simulations at once. This will occupy all the cores of the computer until the simulations are complete. We then output the data into a CSV format that we then analyse in MATLAB. The outputs/detectors allowed in GEANT4 are flexible, which enables for very powerful analysis of almost all aspects of the simulation.

### *3.1 Response Function*

To accurately create the response function, we must first recreate the scintillator array in GEANT4. This includes selecting the correct materials but also adding the additional shielding. Secondly, we must use many input particles and many energies. Typically, this is $10^8$ monoenergetic x-rays with each simulation having input x-ray energies from 1 keV to 100 MeV. It is particularly important to run simulations around the energy region in which the k-edges of the materials is present and other energy regions where the absorption changes by the largest amount.

The output that is analysed from these simulations are usually a position within the scintillator array and a ammount of energy that is despoited. Analysis of this can yield how much energy has been deposited in each layer as a function of input x-ray energy, yielding the desired response functions. Figure 3 a) and b) shows an example of a response function and a fractional absorption graph respectively for 2 mm of LYSO with 2 mm plastic spacing.

### *3.2 X-ray Spectrum Database*

The x-ray spectrum from solid targets primarily depends on three parameters: target material, target thickness and hot-electron temperature. There are several common target materials that are used, however, target thickness and hot-electron temperature can vary by orders of magnitude. This means that many simulations must be conducted to take into account all possible emitted x-ray spectra.

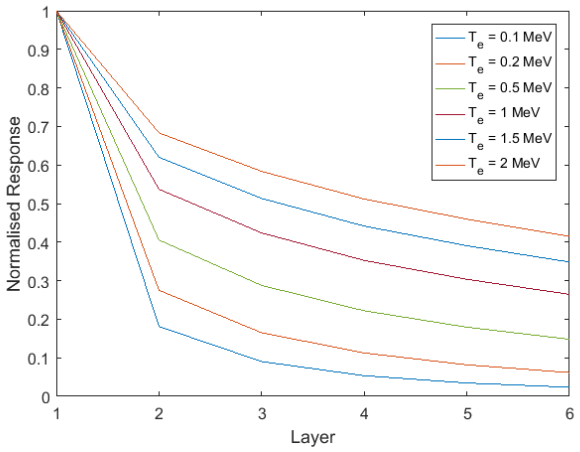


Figure 6: The normalised output of a scintillator array for a number of different temperatures as a function of layer for a 100 $\mu$m Ta target. As the temperature increases, the output becomes shallower.

Here, we demonstrate using a Tantalum target from 10 to 600 $\mu$m and for hot electron temperatures from 10 keV to 2.5 MeV. We know that refluxing will have a major effect on the brightness [12], however, the effect on the spectral shape will be small and the output of the diagnostic will be small [13]. However, to take it into account without having to run numerous simulations, we have recorded the number of electrons that reach the rear surface and the backscattered x-rays. On

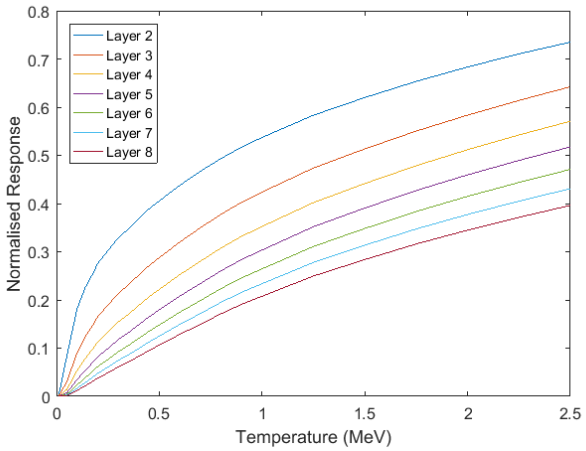


Figure 7: The data plotted in Figure 6 can be plotted as a function of temperature for the different layers. Where the gradients of this curve are largest, the sensitivity to temperature changes is highest.

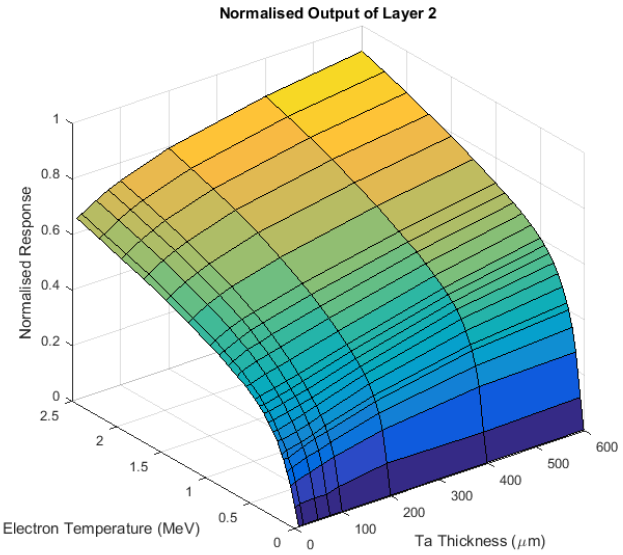


Figure 8: A collection of normalised outputs for layer two as a function of electron temperature and Ta thickness.

the second pass, the backscattered x-ray will be those that contribute to the forward x-ray flux. Therefore, we add this spectrum to the original forward spectrum not before multiplying it by the electron fraction that reaches the rear of the target to take into a account the reduced numbers of electrons.

Figure 4 shows the differences between the outputs from a constant temperature for different thicknesses and vice-versa for Figure 5. The temperature has a much larger effect on the spectral flux and shape in comparison to the thickness of the target.

Multiplying the spectra by the response matrix determines the output of the diagnostic. This will yield an output as a function of layer, which is normalised to the first layer so each output can easily be compared. The output from a 100 $\mu$m Ta target for a number of different temperatures is shown in Figure 6. This highlights the previous point that a 'harder' spectrum will lead to a lower ratio between any layer and the following layer.

This can also be plotted as a function of temperature for different layers as shown in Figure 7. The data displayed in this form allows us to visualise how we would extract the temperature from the data. We can find the best match to a vertical slice through this simulated data and the experimental data; this will correspond to the electron temperature. A discussion of how the comparison is done will be done in following section (4).

As we have conducted simulations for many thicknesses and temperatures, we can produce a 2D plot of the normalised function for any layer, as shown in Figure 8 which is for layer 2 for a Ta target. This more clearly shows the conclusion from Figures 4 and 5 that the output of the diagnostic will change quicker as a function of electron temperature in comparison to the target thickness.

## 4 Temperature Extraction

Finally, we can extract an electron temperature from the diagnostic by comparing the normalised experimental results to the normalised simulation results discussed in Section 3.2.

The simulated and experimental data are compared using the least-squares method. Where the results value form this comparison is maximised (closest to 1), this is considered the temperature. However, we have some uncertainties in the experimental data, this means that we need to repeat this but with different values added to the data to replicate these uncertainties. We can also add some restriction such if the r-squared value is less that a threshold or if with the addition of the uncertainty, the later layers are brighter than the earlier ones.

If we repeat this multiple times, we can create a histogram of temperature where we can retrieve the mean and the standard deviation. An example of this is shown in Figure 9 for a 20 $\mu$m target. Here we have a temperature of approximately 310 keV.

The data obtained from simulations allows us to cycle through target type and thickness so we can retrieve the temperature for many data shots quickly.

## 5 Conclusion

The operation and implementation of the scintillator based spectrometer is explained is detail in this paper. The method behind generating the response function and also the creation of the x-ray spectrum from different targets and input electron spectra using GEANT4 is also discussed. Using the response function and the

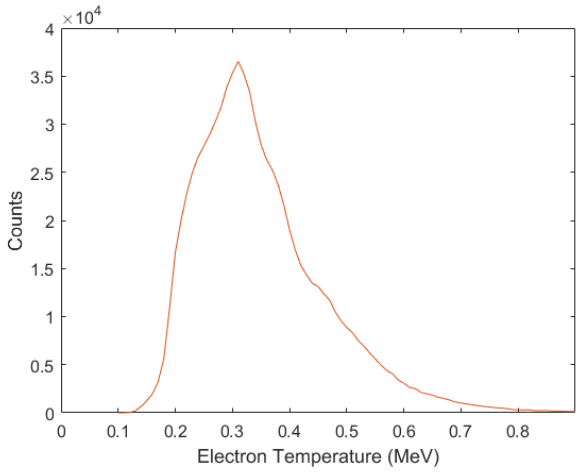


Figure 9: Temperature histogram created from the extraction process from the scintillator diagnostic. The output of the diagnostic is compared to simulation data multiple times, taking into account the uncertainties from the measurement. The temperature (in this case approximately 310 keV) is the mean of this histogram.

spectra, we are able to show how both affect the outputs of the diagnostic in Figure 8.

Finally, we also show how to extract the temperature from the data using a least squares method that is fitted multiple times to take into account the uncertainty of the experimental data.

## References


[1] Mark N Quinn. Investigations of Fast Electron Transport in Intense Laser-Solid Interactions by Declaration of Authorship. 2011.

[2] J. Green, V. Ovchinnikov, R. Evans, K. Akli, H. Azechi, F. Beg, C. Bellei, R. Freeman, H. Habara, R. Heathcote, M. Key, J. King, K. Lancaster, N. Lopes, T. Ma, A. MacKinnon, K. Markey, A. McPhee, Z. Najmudin, P. Nilson, R. Onofrei, R. Stephens, K. Takeda, K. Tanaka, W. Theobald, T. Tanimoto, J. Waugh, L. Van Woerkom, N. Woolsey, M. Zepf, J. Davies, and P. Norreys. Effect of Laser Intensity on Fast-Electron-Beam Divergence in Solid-Density Plasmas. *Physical Review Letters*, 100(1):015003, 2008.

[3] C. D. Chen, J. A. King, M. H. Key, K. U. Akli, F. N. Beg, H. Chen, R. R. Freeman, A. Link, A. J. MacKinnon, A. G. MacPhee, P. K. Patel, M. Porkolab, R. B. Stephens, and L. D. Van Woerkom. A Bremsstrahlung spectrometer using k-edge and differential filters with image plate dosimeters. *Review of Scientific Instruments*, 79(10):2006–2009, 2008.

[4] R. H H Scott, E. L. Clark, F. Pérez, M. J V Streeter, J. R. Davies, H. P. Schlenvoigt, J. J. Santos, S. Hulin, K. L. Lancaster, S. D. Baton, S. J. Rose, and P. A. Norreys. Measuring fast electron spectra and laser absorption in relativistic laser-solid interactions using differential bremsstrahlung photon detectors. *Review of Scientific Instruments*, 84(8), 2013.

[5] John F Seely, Lawrence T Hudson, Glenn E Holland, and Albert Henins. Enhanced x-ray resolving power achieved behind the focal circles of Cauchois spectrometers. *Applied optics*, 47(15):2767–2778, 2008.

[6] D. R. Rusby, C. M. Brenner, C. Armstrong, L. A. Wilson, R. Clarke, A. Alejo, H. Ahmed, N. M. H. Butler, D. Haddock, A. Higginson, A. McClymont, S. R. Mirfayzi, C. Murphy, M. Notley, P. Oliver, R. Allott, C. Hernandez-Gomez, S. Kar, P. McKenna, and D. Neely. Pulsed x-ray imaging of high-density objects using a ten picosecond high-intensity laser driver. 9992:99920E, 2016.

[7] S. Agostinelli, J. Allison, and K. Amako. GEANT4 - a simulation toolkit. *Nuclear Instruments and Methods in Physics Research A*, 506(506):250–303, 2003.

[8] Katsuya Amako, Susanna Guatelli, Vladimir N Ivanchenko, Michel Maire, Barbara Mascialino, Koichi Murakami, Petteri Nieminen, Luciano Pandola, Sandra Parlati, Maria Grazia Pia, Michela Piergentili, Takashi Sasaki, and Laszlo Urban. Comparison of Geant4 electromagnetic physics models against the NIST reference data. *IEEE Transactions on Nuclear Science*, 52(4):910–918, 2005.

[9] L. Pandola, C. Andenna, and B. Caccia. Validation of the Geant4 simulation of bremsstrahlung from thick targets below 3 MeV. *Nuclear Instruments and Methods in Physics Research, Section B: Beam Interactions with Materials and Atoms*, 350:41–48, 2015.

[10] G.A.P. Cirrone, G. Cuttone, F. Di Rosa, L. Pandola, F. Romano, and Q. Zhang. Validation of the Geant4 electromagnetic photon cross-sections for elements and compounds. *Nuclear Instruments and Methods in Physics Research Section A: Accelerators, Spectrometers, Detectors and Associated Equipment*, 618(1-3):315–322, 2010.

[11] S Chauvie, S Guatelli, V Ivanchenko, F Longo, A Mantero, B Mascialino, P Nieminen, L Pandola, S Parlati, L Peralta, M.G. Pia, M Piergentili, P Rodrigues, S Saliceti, and A Trindade. Geant4 low energy electromagnetic physics. In *IEEE Symposium Conference Record Nuclear Science 2004.*, volume 3, pages 1881–1885, 2004.

[12] F. Fiorini, D. Neely, R.J. Clarke, and S. Green. Characterization of laser-driven electron and photon beams using the Monte Carlo code FLUKA. *Laser and Particle Beams*, 32(02):233–241, 2014.

[13] Dean Richard Rusby. *Study of escaping electron dynamics and applications from high-power laser-plasma interactions.* PhD thesis, University of Strathclyde, 2017.